Nuclear Inst, and Methods in Physics Research B 422 (2018) 24–30

Contents lists available at ScienceDirect

Nuclear Inst. and Methods in Physics Research B

journal homepage: www.elsevier.com/locate/nimb

Ion induced electron emission statistics under Ag_m^- cluster bombardment of Ag

A. Breuers*, R. Penning, A. Wucher

Universität Duisburg-Essen, Fachbereich Physik, Lotharstraße 1, 47057 Duisburg, Germany

ARTICLE INFO

Keywords:
Electron statistics
Electron emission
Electronic excitation
Ion bombardment
Yield
Cluster
Silver

ABSTRACT

The electron emission from a polycrystalline silver surface under bombardment with Ag_m^- cluster ions (m = 1,2,3) is investigated in terms of ion induced kinetic excitation. The electron yield γ is determined directly by a current measurement method on the one hand and implicitly by the analysis of the electron emission statistics on the other hand. Successful measurements of the electron emission spectra ensure a deeper understanding of the ion induced kinetic electron emission process, with particular emphasis on the effect of the projectile cluster size to the yield as well as to emission statistics. The results allow a quantitative comparison to computer simulations performed for silver atoms and clusters impinging onto a silver surface.

1. Introduction

A particle impinging onto a solid surface can dissipate its kinetic energy in two different ways, namely via nuclear or electronic stopping. The former describes elastic collision cascades, which can also result in the emission of the surface particles ("sputtering") while the latter describes the interaction of the particle with the electronic system of the solid [1]. The kinetic excitation induced by electronic stopping either of the projectile or of all moving recoil atoms in a collision cascade can lead to excitation or even ionization of the sputtered material as well as to the emission of electrons from the irradiated surface [2]. Particularly the ion induced (kinetic) electron emission has been extensively studied in the past, and an overview of the existing literature can be found in several reviews covering the topic [2–7]. In most of the published work, the surface was bombarded with singly charged atomic ions. Rare gas projectiles were often used in order to avoid any chemical modification of the irradiated surface, since it was found that the emission process may be quite sensitive to surface contamination [6]. Another possibility to avoid projectile induced chemistry is to work under self-irradiation conditions, where an elemental surface is bombarded with projectiles of the same chemical species. This strategy was employed in the present work, which focuses on the kinetic emission of electrons from a polycrystalline silver surface under bombardment with keV silver ions, where nuclear stopping of the projectile clearly dominates. The motivation for using this ion-target combination is that we have done extensive simulations of inelastic processes accompanying the impact of silver atoms and clusters onto a silver surface, which are based on a molecular dynamics treatment of the nuclear motion and include electronic excitation processes by means of simple excitation models. Among other processes like secondary ion formation, these calculations allow a prediction of the kinetic electron emission yield, i.e., the average number of electrons emitted per projectile impact, a quantity which can easily be compared to corresponding experimental data in order to examine the validity of the approximations used in the model calculation. Unfortunately, no data on electron emission are available for this system yet, and the present work is intended to close that gap.

In principle, the electron emission yield, denoted as γ in the following, can be measured by a simple current measurement (CM) method which is described in Section 2.1. A large body of data on kinetic electron emission published to date refers to dependence of this quantity on the kinetic energy of the impinging projectile. From simple kinematical considerations assuming a direct momentum transfer between the projectile and a free electron, it is easy to calculate a classical threshold velocity

$$v_{th} = \frac{1}{2} v_F \left[\sqrt{\left(1 + \frac{\phi}{E_F}\right)} - 1 \right] \tag{1}$$

below which the electron cannot receive enough energy to overcome the surface work function ϕ. For metallic targets and impact velocities larger than v_{th}, the value of γ is often found to scale with the projectile impact velocity, with v_{th} being empirically determined by a linear extrapolation of the data towards the $\gamma = 0$ axis [7]. One of the interesting questions to be addressed in that context refers to the dependence of γ on the nuclearity of a polyatomic projectile. More

* Corresponding author.
E-mail addresses: alexander.breuers@uni-due.de (A. Breuers), andreas.wucher@uni-due.de (A. Wucher).

https://doi.org/10.1016/j.nimb.2018.02.024
Received 15 October 2017; Received in revised form 15 February 2018; Accepted 21 February 2018
Available online 02 March 2018
0168-583X/

specifically, the question arises whether the yield induced, for instance, by the impact of a molecule AB can be described as a linear superposition of the yields induced by the constituents A and B impinging independently with the same velocity. In principle, one might expect the superposition of individual collision cascades induced by particle impacts that are closely correlated in space and time to lead to a very dense collisional spike, which may exhibit emission characteristics different from each cascade alone. In order to address this question, Thum and Hofer [8] developed a concept where metal cluster ions were produced by sputtering, size selected in a quadrupole mass spectrometer and accelerated onto a target surface. They then measured the yield induced by the impact of different Me_m^+ cluster ions at various kinetic energies and found the resulting values, normalized to the number of cluster constituents m, to fall on a universal curve as a function of the cluster impact velocity. Extrapolating the measured data towards zero yield, they determined a threshold velocity of 4.3×10^6 cm/s which is much lower than the classical value calculated using Eq. (1). From these results, the authors concluded that there are no non-linear superposition effects in the kinetic electron emission process, at least in the studied impact energy range with projectile velocities between 8 and 30×10^6 cm/s.

The silver projectiles used in this work are produced in a cluster ion source which – similar to the one used by Thum and Hofer – is based on sputtering. The projectile ions are generated by bombarding a silver target with Cs^+ ions. Under these conditions, negatively charged silver monomers as well as silver clusters are produced, which are accelerated away from the sputter target and focused onto a polycrystalline silver sample surface. Therefore, we can investigate kinetic electron emission under these self-irradiation conditions not only for monoatomic, but also for polyatomic silver cluster projectiles as well. In doing so, we are particularly interested in the low impact energy regime, where the projectile velocity is significantly below the classical threshold value, which for the $Ag{-}Ag$ system with $E_F = 5.5$ eV, $v_F = 1.4 \times 10^8$ cm/s and $\phi = 4.5$ eV is calculated as $v_{th} = 2.3 \times 10^7$ cm/s. For a monoatomic silver projectile ion, this corresponds to a threshold energy of 31 keV, which is significantly above the kinetic energies used here. The projectile ion current delivered by the cluster ion source is large enough to facilitate a measurement of the electron emission yield using the current measuring method. A second source of information regarding the emission process is the statistics, i.e. the probability distribution $P(n)$ for the emission of n electrons during one projectile impact event. In order to determine $P(n)$, it is necessary to reduce the ion current such that one can resolve and distinguish between two subsequent projectiles impinging onto the sample and measure the number n of electrons emitted from that event. To detect the number n, we revert to a technique used extensively at the TU Vienna [8–13] in order to determine the kinetic energy (KE) induced electron emission statistics (EES). Similar experiments have already been done in the past with low kinetic energies but high charge states (e.g. 100 eV Ar^{9+} on gold [13]) to examine the potential energy (PE) induced EES as well. Self-bombardment conditions are used in the present experiments via the irradiation of a polycrystalline silver surface with Ag_m^- cluster ions (m = 1,2,3) in order to facilitate a direct comparison to recent model calculations performed for that system [14]. In particular, we are interested in the effect of the projectile cluster size on the measured yields and emission statistics in order to identify possible non-linear superposition effects arising from the impact of the different cluster constituents.

2. Experimental setup

The experimental setup is depicted in Fig. 1. Heating a Cs^+ ion source provides Cs^+ ions that are accelerated onto a solid target by a voltage V_{Acc}, leading to the sputter emission of singly charged Ag^- and Ag_m^- ions with m = 2–5. Those particles are accelerated as well by V_{Acc} to energies E_P of 5–15 keV, providing the primary Ag_m^- ion beam (sketched as a red arrow in Fig. 1). A Wien filter allows the selection of the cluster size, and electrostatic lenses provide the focussing of the beam, which reaches the polycrystalline sample under an impact angle of 45° with respect to the surface. In order to determine the electron emission yield γ, i.e. the average number of electrons emitted per projectile impact, one can either apply the direct current measurement method (CM) or measure the kinetic energy (KE) induced EES via a solid-state detector. Both methods are subsequently discussed in Sections 2.1 and 2.2, respectively.

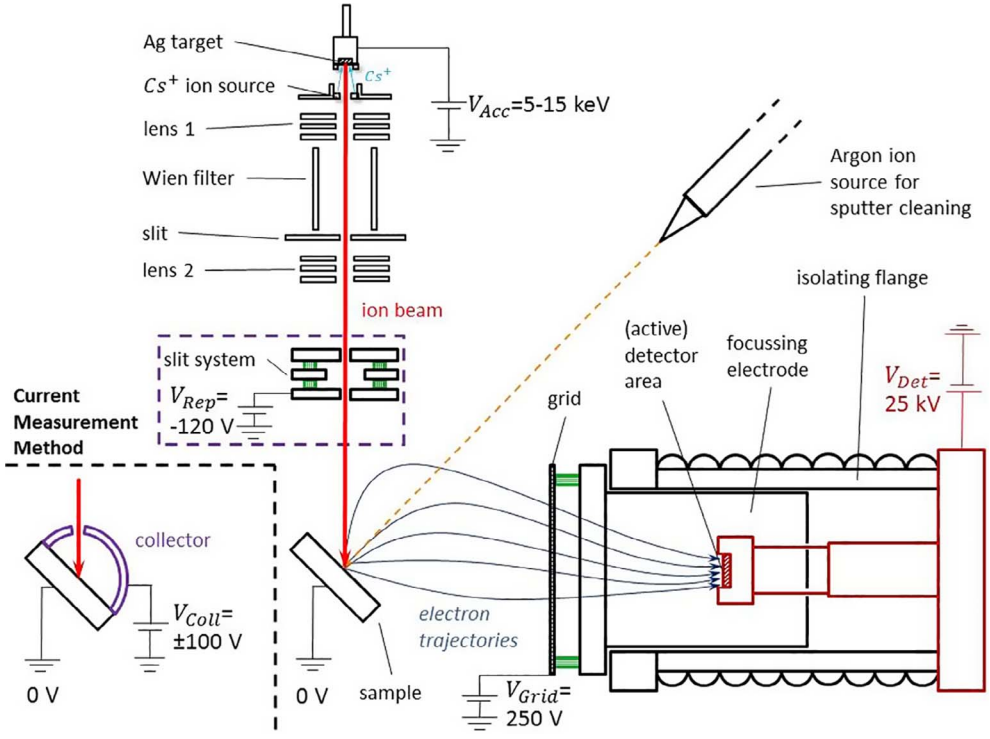

Fig. 1. Experimental setup for either current measurement (CM) method without the slit system (dashed purple box) but a collector (sketched in the bottom left box), or for measurement of the electron emission spectra (EES), including the slit system and the detector unit, sketched on the bottom right area. The same ion beam source is used for both kinds of measurement, providing singly negatively charged Ag_m^- cluster ions with cluster size m in the projectile energy range of E_P = 5–15 keV.

2.1. Current measurement method

For the CM method, the slit system, sketched within the dashed purple box in Fig. 1, is not included, ensuring that the maximum ion current, i.e. ≳3 pA, reaches the sample for sufficiently high signals. Furthermore, the setup is equipped with a collector (sketched in purple in the bottom left corner in Fig. 1) which is electrically isolated from the sample, so that a bias voltage V_{Coll} of ± 100 V with respect to the sample potential can be applied to it. A positive bias voltage assures that emitted secondary electrons are repelled back to the sample, hence not contributing to the measured sample current. On the other hand, a negative bias voltage ascertains that those electrons in fact do contribute to the signal as an electron current leaving the sample. Setting those two measurements into relation, one can obtain the yield γ by

$$\gamma = \frac{I_M^+ - I_M^-}{I_M^-}, \tag{2}$$

where $I_M^{+/-}$ denotes the measured current on the sample for a positively/negatively biased collector.

2.2. Electron emission statistics method

For the EES measurement, the slit system is inserted into the beamline, thereby reducing the projectile ion current to sufficiently small values, i.e. ≲8 fA, to ensure that individual projectile impacts are sufficiently spaced in time, so that the capability of the silicon detector to process a maximum of 5×10^4 events per second is not surpassed. Two potentials, $V_{Rep} = -120$ V and $V_{Grid} = 250$ V, allow the manipulation of the electron trajectories onto the detector unit, where a high detector potential $V_{Det} = 25$ kV and a grounded electrode focus the electrons onto the active area of the detector. A number of n simultaneously impinging electrons following a projectile impact ("event") generates a pulse signal n times higher than a single electron, thus a time-integrated histogram of many electron emission events results in a spectrum of counts vs channel, where the channel number is proportional to the electron number n. Consequently, the full EES can be obtained and the yield can be extracted from the data.

It is necessary to use such high detector potentials to overcome the limited resolution of the detector of $\Delta E_{Det} = 6.9$ keV. At the same time, high voltages increase the risk of arcing and field emission. Thus, a voltage of $V_{Det} = 25$ kV is a good agreement between sufficient resolution and technical stability.

In addition to the cluster projectile ion source, an Ar^+ sputter gun was used for cleaning the target metal surface of the sample with impact energies of ≳10 keV and ion currents of ≳600 nA. Furthermore, the experiment was conducted in an UHV chamber with a base pressure of 2.5×10^{-8} mbar, thereby providing sufficient mean free path lengths of the emitted electrons to reach the detector.

3. Data acquisition and evaluation of the electron emission statistics

Fig. 2 exemplifies the raw counts vs channel data obtained for the bombardment of a sputter cleaned polycrystalline silver surface with 9 keV Ag_1^- projectiles under an impact angle of 45° with respect to the surface normal. While a "channel" refers to the output signal of the silicon detector (in arbitrary units), each "count" refers to an event in which a particular output signal was recorded.

One can clearly distinguish between the peaks corresponding to the simultaneous detection of $n = 1,2,3,...$ electrons and thus determine the probability of these events via the amplitude of the respective peak. However, two circumstances have to be taken into account. First, for the background of the spectra, the inelastic backscattering of the electrons at the detector must be considered, as already explained in detail in [9] and [12]. This effect can be described by the polynomial

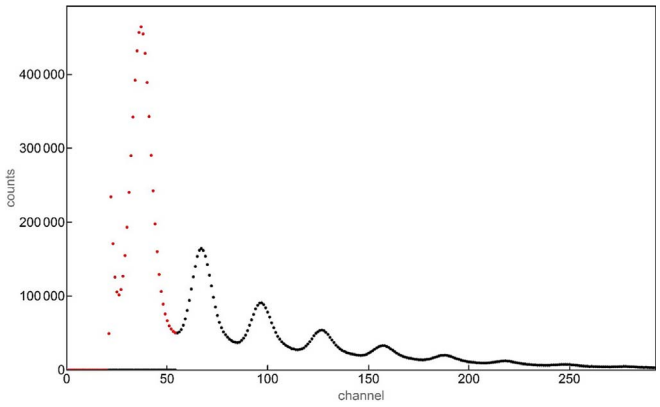

Fig. 2. Presentation of the measured data counts vs channel. The peaks for $n = 1,2,3,...$ electrons are clearly distinguishable. The first peak, displayed as red dots, is neglected during further analysis of the spectra due to electron detachment (ED) of the incident ion impinging onto the surface.

distribution

$$P(n,k,p) = \binom{n}{k} p^k (1-p)^{n-k} \tag{3}$$

describing the probability for inelastic backscattering of k electrons out of a group of n electrons impinging initially onto the active detector area. Each individual electron is backscattered with a probability p and can then be accelerated back onto the active detector area and contribute to the signal at lower energies (e.g. more left in the spectra) of ~60% of their initial impact energy [9,12], the latter corresponding to the electron acceleration voltage V_{Det}. Furthermore, the FWHM ΔE_k of the backscattered electron peak can be calculated by convoluting the energetic detector resolution $\Delta E_{Det} = 6.9$ keV with the FWHM $\Delta E \approx 12$ keV [9,12] of the statistical distribution (which is assumed to be Gaussian-shaped), leading to a width of the k-th backscattered electron peak according to

$$\Delta E_k = \sqrt{(\Delta E_{Det})^2 + k(\Delta E)^2}. \tag{4}$$

Here, for each group of n electrons, the first two terms for k are taken into account to describe the background sufficiently and the corresponding ΔE_k are considered as fitting parameters; the influence for k ≥ 3 is negligible. Simulations using the program SIMION estimated the probability $p \approx 12$–16%, which conforms with [15] very well. Knowing these parameters quite well allows the fitting of the peaks in the spectra as well as the area between, as Fig. 3 confirms.

Second, the effect of electron detachment (ED) distorts the result for the yield γ. ED describes the weakly bound electron from the singly charged projectile to become unbound upon impact of the projectile ion onto the sample and hence contribute to the measurement of the EES. Since it is not possible to distinguish between solid state electrons and electrons from the projectile, the weakly bound electron from the Ag_m^- projectile adds to the signal measured at $n = 1$ whenever an incident neutral (or positive ion) projectile would rather emit no electrons (with the probability $P(0)$). As a consequence, the electron peak measured for $n = 1$ is significantly overestimated. To avoid the resulting distortion in evaluating the EES, the first peak, displayed as red dots in Fig. 2, is completely ignored in the following analysis of the spectra.

Considering these two effects, Fig. 3 finally depicts the reproduction of the measured spectra (black dots) for $n \geq 2$ by fitting each individual peak with a Gaussian shape (solid lines) and their respective backscattered peaks (dashed lines). This allows the analysis of the emission probabilities $P(n)$ as well as the appropriate yield γ by matching a distribution function to them.

One might notice the very good agreement of the measured data curve (black dots in Fig. 3) by the summed fit functions (black solid line in Fig. 3), revealing the maxima of the electron peak as well as the

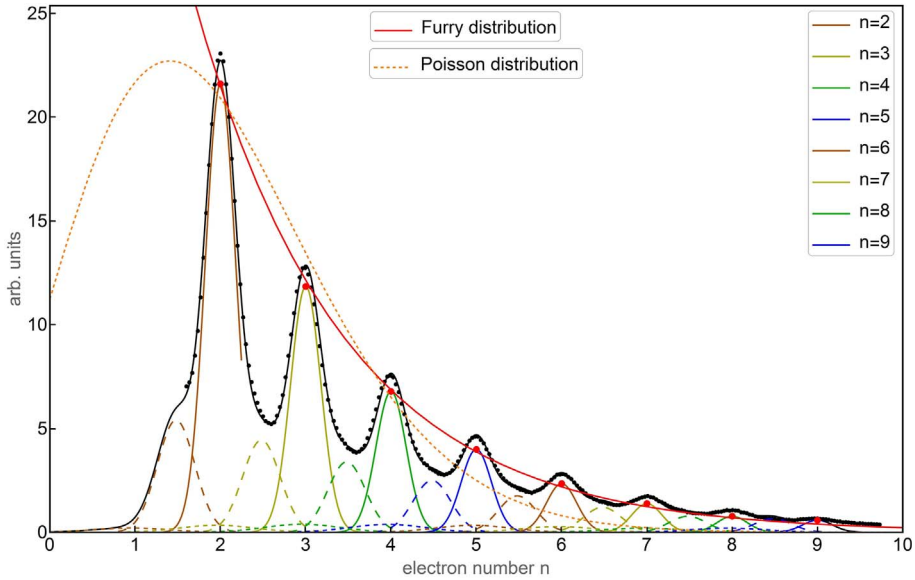

Fig. 3. Fitting of the spectra with Gaussian shaped peaks (solid line) and their respective backscattered peaks (dashed lines). This way, the spectra can be reproduced excellently, covering both the peaks and the structure between them. Thus, a Furry distribution, as well as a Poisson distribution for comparison, is mapped onto the data to evaluate the yield γ.

structures in between. This enables the mapping of a statistical distribution function to the maxima, which is commonly a Poisson distribution [16]. Apparently, Fig. 3 shows clear deviations between the best fit of a Poisson distribution, indicated as a dotted orange line in Fig. 3, and the measured data. However, the data suggest an exponential decay, which can be described by the so-called Furry distribution

$$P_F(n,\mu) = \frac{\mu^n}{(1+\mu)^{n+1}} \tag{5}$$

with a fitting parameter μ [17]. The best fit of this function is indicated by the solid red line in Fig. 3. It is seen that the Furry distribution can describe the measured data almost exactly. Since the expectation value of the number n given by any probability distribution P (n) equals the average emission yield γ, and the corresponding expectation value given by the Furry distribution equals the parameter μ, the fit function for $P_F(n,\mu)$ delivers directly the yield $\gamma \equiv \mu$. For the example shown in Fig. 3, the resulting yield is $\gamma = 1{,}27 \pm 0{,}027$ electrons/ion. The yield values determined this way can be compared to the results obtained from the CM method, which will be discussed below in Section 4.1.

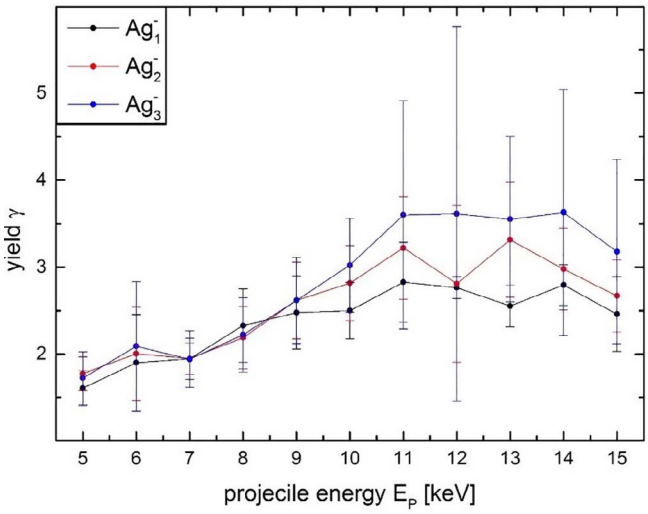

Fig. 4. Measured yield γ as a function of the projectile energy E_P. An ascending trend can be identified for all three cluster sizes Ag_m^-, as well as a plateau for $E_P \geq 11$ keV. The yield ranges between 1.5 and 3.5. The error bars result from the standard deviation of the average of six measurements for each data point.

4. Results

4.1. Current measurement method

The electron emission yields γ determined by the current measurement method are depicted in Fig. 4 as a function of the projectile energy E_P for three different kinds of projectiles Ag_m^- (m = 1,2,3). The displayed data represent the average result of six independent measurements for each point, and the depicted error bars correspond to the standard deviation of this average. At low impact energy, the measured yield appears to be independent of the projectile cluster size, while an increase with increasing cluster size is observed at higher impact energies. For all projectiles, the yield γ is found to increase with increasing projectile energy E_P, until for $E_P \geq 11$ keV the yields appear to level off. The deviation from a completely rising trend can be explained by possible contributions of secondary or tertiary particles leaving or impinging onto the sample, e.g. from the collector. Typically, these are neglected in the determination of γ in Eq. (2), but could affect the measurement significantly. It is furthermore remarkable that the absolute yield values range between 1.5 and 3.5 emitted electrons per incident projectile ion. In interpreting this result, the effect of electron detachment has to be taken into account, as the negative charge state of the projectile almost certainly adds an electron to the measured yield, thus overestimating the actual kinetic electron emission yield by approximately 1. In order to correct for this effect, one has to either artificially lower the measured yield by 1 or determine γ by the expectation value of the electron emission spectra. A comparison with the evaluated yields from the EES in Fig. 5 will show sufficient agreement, thus the estimation to decrease the measured yield by 1 is probably justified.

4.2. Electron emission statistics

The resulting electron emission spectra produced under bombardment with Ag_1^- projectiles are shown in Fig. 5 for different values of the primary ion energy E_P. The emission probability $P(n)$ decreases exponentially with the electron number n. It is worth noting that the

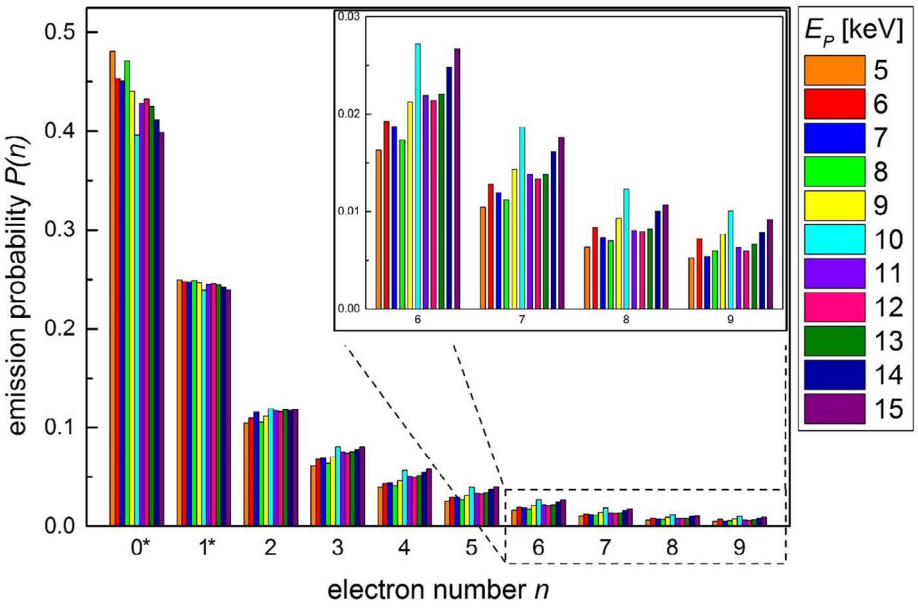

Fig. 5. Emission probabilities $P(n)$ as a function of the electron number n for projectile energies E_P according to the colour scale on the right. The probabilities $P(0)$ an $P(1)$ (denoted with a "*") are calculated from the Furry distribution fitted to the remaining $P(n)$. A clear ascending trend of the individual probabilities for each electron number $n \geq 2$ can be seen for rising projectile energies E_P.

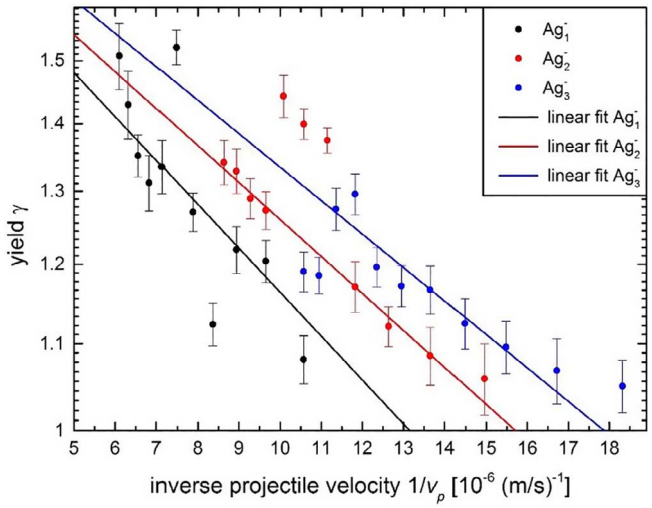

Fig. 6. Evaluated yield γ vs inverse projectile velocity $1/v_P$. The yields range between 1.0 and 1.5 and are solely decreasing for larger $1/v_P$, both aspects contrasting the results of CM method in Fig. 4. The spreading of the straight lines in this view suggest already an effect of the cluster size in the electron emission (otherwise the lines would be identical), as is subsequently discussed in detail.

displayed probabilities $P(0)$ and $P(1)$ for emission of either no or one electron have been extrapolated according to the Furry distribution as explained above, and are therefore denoted with a "$*$". Inspecting the data, a clearly ascending trend can be discovered for each of the probabilities $P(n)$ with $n \geq 2$ for rising E_P. Consequently, the contribution to $P(0)$ decreases accordingly, whereas $P(1)$ remains nearly constant. This suggests that the electron yield lies in the order of $\gamma \gtrsim 1$, which can be verified in Fig. 6. There is, however, a scatter around these overall trends which is most notable for the data measured at $E_P = 10$ keV. Although we tried to properly clean the target surface prior to each measurement using prolonged Ar^+ ion sputtering, the excessive probabilities $P(n)$ observed for $n \geq 3$ at this energy may possibly arise from a slightly larger residual surface contamination at this energy, which might act to enhance the average emission yield.

Since the projectile velocities used here are clearly beneath the threshold velocity v_{th} for ballistic electron emission from silver (2.3×10^7 cm/s, see above) [18], sub-threshold electron emission models have to be used for comparison with the measured yields, which predict the number of kinetically excited hot electrons with large enough excitation energy to overcome the surface work function. Published models generally describe the dependence of the yield resulting from collective excitation of the conduction band electron gas on the velocity v_P of the impinging projectile as

$$\gamma(v_P) \propto v_P \times \exp\left(-\frac{\alpha}{v_P}\right), \tag{6}$$

with α being a constant containing the work function of the solid and either an inverse decay length according to the surface-assisted kinetic electron emission model [19] or an elevated electron temperature due to the excitation mechanism described in the hot-spot model [20]. Those predictions suggest a semi logarithmic plot of γ over $1/v_P$, as presented in Fig. 6. Here, the first term, $log(v_P)$, can safely be neglected, as almost only the second term, $-(\alpha/v_P)$, describes the characteristics of the function in Eq. (6) due to the dominant exponential term for small v_P (and thus for sufficiently large $1/v_P$ in the portrayal in Fig. 6). In order to visualize the velocity dependence of the measured yields, linear least square fits according to the prediction of Eq. (6) are included in Fig. 6. Although these fits could in principle be used to determine the parameter α, we refrain from such an analysis here since the fits appear to be highly questionable due to the large scatter of the data. Nevertheless, the three clearly separated fit lines indicate that for a given projectile impact velocity the yields are generally higher with increasing projectile cluster size.

The yield values range between 1.0 and 1.5, and exhibit an overall decreasing trend for larger $1/v_P$ (hence increasing for larger v_P), which contrasts the yields determined by the CM method in Fig. 4. This is owed to the fact that the electron detector used in the EES measurement receives no secondary or even tertiary particles, but only the emitted electrons from the sample. It allows the analysis of γ without considering those particles distorting the measurement. The representation of the yield over the inverse projectile velocity allows a comparison of the yield for the different cluster sizes as well, which is motivated briefly in the following.

As the particles of an ion beam basically never hit the sample at the

Table 1
Presentation of the yields $\gamma \pm \Delta\gamma$ for the same energy per nucleus (5 keV per Ag atom) in the cluster. An effect of the cluster size can clearly be observed in the values of γ, yet its increase proceeds sub-linear with increasing number of atoms in the cluster m.

	γ	$\Delta\gamma$
Ag_1^-	1,16	0,032
Ag_2^-	1,26	0,029
Ag_3^-	1,31	0,019

same time or space (compared to excitation times and volumes), only clusters ensure that two or more atoms hit the surface simultaneously. This gives rise to the question whether the individual particles dissipate their energy independently. If the effects induced by each projectile constituent would superpose in a linear fashion, the yield measured for an Ag_m cluster projectile should simply be m times that measured for Ag_1 at the same impact velocity. A quantitative analysis of linearity can therefore be made by comparing γ for the same energy per nucleus, i.e. 5 keV per atom in the cluster, which relates to about $10.5 \times 10^{-6}(\mathrm{m/s})^{-1}$. Table 1 illustrates a clear sub-linear behaviour of the yield with increasing cluster size, i.e.:

$$\gamma(Ag_m^-) < m \times \gamma(Ag_1^-) \tag{7}$$

From sputtering experiments, it is found that the non-linear superposition of collision cascades induced by each cluster constituent leads to a very dense collisional spike, which produces a non-linear enhancement of the sputter yield induced by a cluster projectile [21]. The data presented in Table 1 show that this effect does not occur for the kinetic electron emission accompanying the nuclear dynamics. In that sense, the results obtained here are in qualitative agreement with the data measured by Thum and Hofer [8], who found a strictly linear additivity of the electron yields induced by impact of V_m^+ and Nb_m^+ cluster ions onto a stainless steel surface. Interestingly, the results determined here even point in the opposite direction, indicating a *sub-linear* additivity under impact of Ag_m^- ions onto silver. There are two significant differences between the experiments of Thum and Hofer and those performed here. First, the projectile charge state may in principle influence the measured yields. For the case of positive ions, this is in principle possible by a potential emission process, provided the projectile ionization potential is larger than twice the surface work function [6]. Since the ionization potential of different clusters is different, this contribution may vary as a function of projectile cluster size. Moreover, a careful analysis of the detection probabilities of large silver clusters on a microchannel plate at different post-acceleration voltages have revealed that there must be a significant contribution to the electron emission yield which is independent of the impact velocity even if the potential emission criterion is not fulfilled [22]. For the case of negative ions, on the other hand, we are faced with the electron detachment problem described above, which must in principle be corrected for if the true, kinetically induced emission yield is to be determined. Second, the data taken by in Ref. [8] were taken at higher impact energies than used here. Their data indicate a threshold velocity for kinetic electron emission, which is much lower than what would be expected from Eq. (1), but indicates that their experiments were clearly performed in the above-threshold region. The measurements performed here, on the other hand, clearly reside in the sub-threshold region, where the physical mechanisms of kinetic electron emission might be different.

Looking at the values presented in Table 1, one should keep in mind that the yields are evaluated for an impact angle of $\theta = 45°$, which is caused by our basic experimental geometry. For comparison with perpendicular impact, those yields should be corrected by a factor of $\cos^f\theta$, where f is an exponent slightly different from unity [23]. For $\theta = 45°$, those considerations would lead to yields reduced by a factor of $1/\sqrt{2}^f$ for perpendicular projectile impact, which has been done (for $f = 1$) to subsequently compare the measurements to computer simulations.

4.3. Comparison with computer simulations

Finally, both results are compared to recent computer simulations, which predict the yield γ for the bombardment of an $Ag(111)$ surface with Ag_1 [14]. The simulations are based on molecular dynamics simulations of the collision cascade initiated by the projectile impact. The resulting nuclear dynamics are coupled to the electronic degrees of freedom by the fact that all particles moving in the solid experience electronic stopping, which is implemented into the calculations by means of an electronic friction term and an excitation probability in close, violent atomic collisions. The transport of the excitation energy generated this way is treated in terms of a non-linear diffusive approach, with the excitation energy density being parametrized in terms of a locally enhanced electron temperature and the electronic heat diffusivity being allowed to depend on both the electron temperature and the local lattice disorder generated within the collision cascade. The spatio-temporal electron temperature profile calculated this way is then inserted into a Richardson-Dushman-type thermionic emission equation, and the resulting electron flux across the surface barrier is integrated to deliver the electron emission yield. It is crucial to test the yields calculated with such a microscopic emission model against experimental data. For computational reasons, the simulations were performed for a self-bombardment system, where the interaction of the target and projectile atoms was described in terms of a parametrized many-body potential fitted to the properties of solid silver. In order to test the approximations behind the excitation and emission model, it is mandatory to compare the computed yield values against corresponding experimental data. In order to particularly describe the electron emission in the sub-threshold energy range, the calculations were performed for impact energies between 100 and 1000 eV, where experimental data is extremely scarce. Comparing the results with data taken for Xe^+ ions impinging on gold, we found a similar impact energy dependence, albeit the yield values calculated for the same impact velocity were by about a factor 5 too large. At the time of the publication of the paper, it was debated whether this discrepancy was due to the different ion-target system or rather indicated a problem of the calculation. Since the calculations cannot easily be extended to other projectile-target combinations, it appeared necessary to obtain experimental yield data for the self-irradiation Ag–Ag system and compare those with the calculated data. The result is shown in Fig. 7.

Even though the calculations were mostly performed at lower impact energies than the ones used here, there is an overlap at an impact energy of 1 keV, corresponding to 0.05 keV/amu, where predicted and measured yield values can be compared. It is seen that particularly the yield determined from the measured electron emission statistics agrees almost perfectly with the calculated value, lending credibility to the emission model behind the calculated values. The yield measured by the CM method is by a factor < 2 larger, a finding which is expected due electron detachment problem induced by the negative charge state

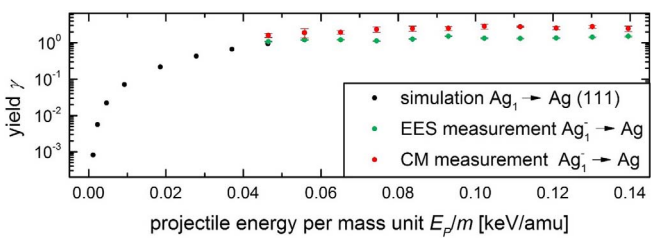

Fig. 7. Comparison of the measured yields with simulated γ for Ag_1 projectiles bombarding an $Ag(111)$ surface [14]. The transition at 0.05 keV/amu for EES as well as for CM seems rather plausible; the measurements with EES provide a better overlap though. However, a good agreement between simulation and experiment can be observed.

of the projectile ions as explained above. It suggests the physical assumptions for the simulation to be correct, which then motivates to excess the simulation range to greater projectile energies as well as the measurement range to lower ones. However, this presumes larger capacities for calculation or stability of the ion source for $E_P < 5\,\mathrm{keV}$. Currently, the results from the EES measurement seem rather plausible, are in good agreement with simulations and even allow the observation of the cluster effect for Ag_m^- cluster.

5. Conclusion

In this work, the ion induced kinetic electron emission produced by silver projectiles impinging on a silver surface is measured by two different experimental methods. A slight deviation in the evaluation of the respective yields determined from the conventional current measuring method and the electron emission statistics, which can be explained by the negative charge state of our projectile ions, leading to effective detachment of the excess electron upon projectile impact. It is shown that this effect affects both measurement methods in a different way, and can be efficiently corrected by comparing the measured emission statistics to the well-known Furry distribution. Comparing the results obtained for Ag_m^- projectiles with $m = 1,2,3$, a sub-linear cluster effect is identified by the analysis of γ as a function of projectile energy and cluster size, where the yield measured for cluster projectile is smaller than the sum of the yields induced by the independent impact of its constituents with the same velocity.

Moreover, the results obtained here deliver badly needed experimental data to compare to recent computer simulations of the electronic excitation accompanying a collision cascade initiated by the projectile impact and the kinetic electron emission resulting from it. We find that the experimental yield values measured here are in good agreement with those determined from the microscopic emission model, with the yields determined from the measured electron emission statistics fitting almost perfectly to the calculated data. This agreement lends credibility to the various simplifications and approximations used in the model calculations, thereby giving hope for future developments of a microscopic model describing excitation and ionization during ion bombardment of solid surfaces.

References

[1] C. Heuser, M. Marpe, D. Diesing, A. Wucher, Kinetic excitation of solids induced by energetic particle bombardment: influence of impact angle, Nucl. Instrum. Methods B 267 (2009) 601–604.

[2] R.A. Baragiola, Principles and mechanisms of ion induced electron emission, Nucl. Instrum. Methods B 78 (1993) 223–238.

[3] B.A. Brusilovsky, Directional effects in kinetic ion-electron emission, Vacuum 35 (1985) 595–615.

[4] B.A. Brusilovsky, Kinetic ion-induced electron emission from the surface of random solids, Appl. Phys. A 50 (1990) 111–129.

[5] S.R. Kasi, H. Kang, C.S. Sass, J.W. Rabalais, Inelastic processes in low-energy ion-surface collisions, Surf. Sci. Rep. 10 (1989) 1–104.

[6] W.O. Hofer, Ion-induced electron emission from solids, Scanning Microsc. 4 (1990) 265–310.

[7] R.A. Baragiola, Electron emission from slow ion-solid interactions, in: J.W. Rabalais (Ed.), Low Energy Ion-Surface Interactions, Wiley & Sons, Chichester, 1994, pp. 187–262.

[8] F. Thum, W.O. Hofer, Non enhanced electron emission from high-density atomic collision cascades in metals, Surf. Sci. 90 (1979) 331–338.

[9] G. Lakits, F. Aumayr, H. Winter, Statistics of ion-induced electron emission from a clean metal surface, Rev. Sci. Instrum. 60 (1989) 3151–3159.

[10] G. Lakits, F. Aumayr, H. Winter, Statistics of potential electron emission, Radiat. Eff. Defects Solids 109 (1989) 129–136.

[11] F. Aumayr, T.D. Mark, H. Winter, The statistics of electron emission from clean metal surfaces induced by slow ions: measurement and recent applications, Int. J. Mass Spectrom. Ion Phys. 129 (1993) 17–29.

[12] F. Aumayr, G. Lakits, H. Winter, On the measurement of statistics for particle-induced electron emission from a clean metal surface, Appl. Surf. Sci. 47 (1991) 139–147.

[13] D. Schrempf, W. Meissl, F. Aumayr, An ultra-compact setup for measuring ion-induced electron emission statistics, Nucl. Inst. Methods Phys. Res., B 317 (2013) 44–47.

[14] A. Duvenbeck, B. Weidtmann, A. Wucher, Predicting kinetic electron emission in molecular dynamics simulations of sputtering, J. Phys. Chem. C 114 (2010) 5715–5720.

[15] H. Drescher, L. Reimer, H. Seidel, Rückstreukoeffizient und Sekundärelektronen-Ausbeute von 10-100 keV-Elektronen und Beziehungen zur Raster-Elektronenmikroskopie, Z. angew. phys. (1970).

[16] L.A. Dietz, J.C. Sheffield, Spectrometer for measuring secondary electron yields induced by ion impacts on thin film oxide surfaces, Rev. Sci. Instrum. 44 (1973) 183–191.

[17] F. Thum, Ion-Induced Electron Emission from Gold Surfaces, MPI Garching, 1979, pp. 31–33.

[18] R.A. Baragiola, E.V. Alonso, J. Ferron, A. Oliva-Florio, Ion-induced electron emission from clean metals, Surf. Sci. 90 (1979) 240–255.

[19] J. Lorincik, Z. Sroubek, M. Brunmayr, G. Kowarik, F. Aumayr, Kinetic electron emission due to perpendicular impact of carbon ions on tungsten surfaces, Appl. Surf. Sci. 255 (2009) 6303–6307.

[20] Z. Sroubek, Kinetic electron emission from metals induced by impact of slow atomic particles, Nucl. Instrum. Methods B 268 (2010) 3377–3380.

[21] S. Bouneau, A. Brunelle, S. La-Negra, J. Depauw, D. Jacquet, Y. Le Beyec, M. Pautrat, M. Fallavier, J.C. Poizat, H.H. Andersen, Very large gold and silver sputtering yields induced by keV to MeV energy Au_n clusters (n = 1-13), Phys. Rev. B 65 (2002) 144106.

[22] P. Mazarov, Charakterisierung eines Flugzeit-Massenspektrometers und seine Anwendung in der Festkörper-Oberflächenuntersuchung, Universität Duisburg-Essen, 2006 (Ph.D. thesis).

[23] J. Ferron, E.V. Alonso, R.A. Baragiola, A. Oliva-Florio, Dependence of ion-electron emission from clean metals on the incidence angle of the projectile, Phys. Rev. B 24 (1981) 4412.